



Off-axis optical vortices using double-Raman singlet and doublet light-matter schemes

Hamid Reza Hamedi ^{1,*}, Julius Ruseckas^{1,†}, Emmanuel Paspalakis ^{2,‡} and Gediminas Juzeliūnas ^{1,§}

¹*Institute of Theoretical Physics and Astronomy, Vilnius University, Saulėtekio 3, Vilnius LT-10257, Lithuania*

²*Materials Science Department, School of Natural Sciences, University of Patras, Patras 265 04, Greece*



(Received 28 January 2020; accepted 1 June 2020; published 22 June 2020)

We study the formation of off-axis optical vortices propagating inside a double-Raman gain atomic medium. The atoms interact with two weak probe fields as well as two strong pump beams which can carry orbital angular momentum (OAM). We consider a situation when only one of the strong pump lasers carries an OAM. A particular superposition of probe fields coupled to the matter is shown to form specific optical vortices with shifted axes. Such off-axis vortices can propagate inside the medium with sub- or superluminal group velocity depending on the value of the two-photon detuning. The superluminal optical vortices are associated with the amplification as the energy of pump fields is transferred to the probe fields. The position of the peripheral vortices can be manipulated by the OAM and intensity of the pump fields. We show that the exchange of optical vortices is possible between individual probe beams and the pump fields when the amplitude of the second probe field is zero at the beginning of the atomic cloud. The model is extended to a more complex double Raman doublet interacting with four pump fields. In contrast to the double-Raman-singlet, now the generation of the off-axis sub- or superluminal optical vortices is possible even for zero two-photon detuning.

DOI: [10.1103/PhysRevA.101.063828](https://doi.org/10.1103/PhysRevA.101.063828)

I. INTRODUCTION

Electromagnetically induced transparency (EIT) [1,2] is an optical effect in which the susceptibility of a weak probe field is modified for an optically thick three-level Λ atomic system. The medium becomes transparent for the probe transition by applying a stronger control field driving another transition of the Λ system. A number of important phenomena [3–6] rely on the EIT, including adiabats [7–9], matched pulses [10,11], giant optical nonlinearities [9,12–15], and optical solitons [16,17]. Due to the EIT the light pulses can be slowed down [1,2,18–24] and also stored in the atomic medium by switching off the controlled laser [19,25–28]. This can be used to store the quantum state of light to the matter and back to the light leading to important applications in quantum technologies [19,29,30].

In parallel, there have been important efforts dedicated to the superluminal propagation of light pulses in coherently driven atomic media [31–34]. An anomalous dispersion leading to the superluminal propagation can be naturally obtained within the absorption band medium [35] or inside a tunnel barrier [36]. Yet such a superluminal propagation is hardly observed due to losses [35]. Some novel approaches have been proposed to utilize transparent spectral regions for fast light [37–41]. Specifically, it was shown that a linear anomalous dispersion can be created in a Raman gain doublet and therefore distortionless pulse propagation is possible [38].

Vortex beams of light [42–44] representing an example of the singular optics are of the fundamental interest and offer many applications [6,23,45–65]. The optical vortices are described by a wave field whose phase advances around the axis of the vortex and the associated wavefront carries an orbital angular momentum (OAM) [42–44]. The phase of the on-axis optical vortices advances linearly and monotonically with the azimuthal coordinate reaching a multiple of 2π after completing a closed circle around the beam axis. When two twisted beams each carrying an optical vortex are superimposed, the resulting beam contains new vortices depending on the charge of each vortex component [60,66–68]. Besides the on-axis vortices, the off-axis optical vortices can be formed for which the vortex core is not on the beam axis but moves about it [68–72].

In this article we propose a scenario for formation of off-axis optical vortices in a four-level atom-light coupling scheme. We consider a double-Raman gain medium interacting with two weak probe fields, as well as two stronger pump laser beams which can carry the OAM. A specific combination of the probe fields is formed with a definite group velocity determined by the two-photon detuning. Note that the individual probe beams do not have a definite group velocity when propagating inside the medium. If one of the pump laser beams carries an optical vortex, the resulting superposition beam exhibits off-axis vortices propagating inside the medium with a sub- or superluminal group velocity depending on the two-photon detuning. The position of the peripheral vortices around the center can be manipulated by the OAM and the intensity of the pump fields. It is shown analytically and numerically that the OAM of the pump fields can be transferred to the individual probe beams when the amplitude of the second probe field is zero at the beginning of the medium. We also extend the model to a more complex

*hamid.hamedi@tfai.vu.lt

†julius.ruseckas@tfai.vu.lt

‡paspalak@upatras.gr

§gediminas.juzeliunas@tfai.vu.lt

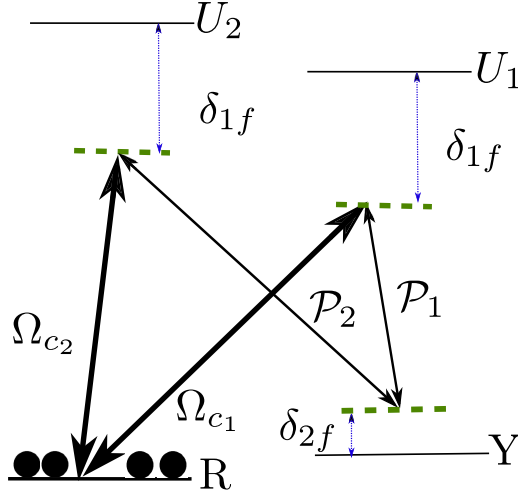


FIG. 1. Schematic diagram of the double Raman scheme.

double Raman doublet scheme interacting with four pump fields.

The paper is organized as follows. In the next section we consider the light propagation using a double Raman scheme and show that off-axis optical vortices with either slow or fast light properties can be created. In Sec. III we extend the model by considering formation of the off-axis optical vortices occurring under the slow or fast light propagation in the double Raman doublet scheme. Our results are summarized in Sec. IV.

II. DOUBLE-RAMAN SCHEME

Let us consider propagation of two probe fields in an atomic medium with the Raman gain described by the double Raman scheme illustrated in Fig. 1. The atoms forming the medium are characterized by two hyperfine ground levels R and Y and two electronic excited levels U_1 and U_2 . The quantum state of the atoms is described by the probability amplitudes $\Psi_{\mathbf{R}}(\mathbf{r}, t)$, $\Psi_{\mathbf{Y}}(\mathbf{r}, t)$, $\Psi_{U_1}(\mathbf{r}, t)$, and $\Psi_{U_2}(\mathbf{r}, t)$ normalized to the atomic density n : $|\Psi_{\mathbf{R}}|^2 + |\Psi_{\mathbf{Y}}|^2 + |\Psi_{U_1}|^2 + |\Psi_{U_2}|^2 = n$.

The atoms interact with two weak probe fields with slowly varying amplitudes \mathcal{P}_1 and \mathcal{P}_2 , as well as two strong pump lasers. The Rabi frequencies of the pump fields can be generally expressed as

$$\Omega_{c_j} = \mathcal{E}_{c_j}(r)e^{il_j\varphi}, \quad (1)$$

where

$$\mathcal{E}_{c_j}(r) = |\Omega_{c_j}|(r/w)^{|l_j|}e^{-r^2/w^2} \quad (2)$$

is a fundamental Gaussian beam for $l_j = 0$, while it describes a Laguerre-Gaussian (LG) doughnut beam when $l_j \neq 0$. Here φ is the azimuthal angle, r describes the cylindrical radius, w denotes the beam waist parameter, and $|\Omega_{c_j}|$ ($j = 1, 2$) is the strength of the pump beam.

The atoms are assumed to be initially in the ground level (Raman level) R . The Rabi frequency and duration of the probe pulses are small enough, so that the depletion of the ground level R is neglected. We work under the four-photon

resonance condition $\omega_{p_1} - \omega_{c_1} = \omega_{p_2} - \omega_{c_2}$, where ω_{p_1} and ω_{p_2} are the frequencies of the probe beams and ω_{c_1} and ω_{c_2} are the frequencies of the pump beams.

After introducing the slowly varying atomic amplitudes we obtain the following equations for slowly varying probe fields:

$$(\partial_t + c\partial_z)\mathcal{P}_1 = i\alpha_1\Phi_Y^*\Phi_{U_1}, \quad (3)$$

$$(\partial_t + c\partial_z)\mathcal{P}_2 = i\alpha_2\Phi_Y^*\Phi_{U_2}, \quad (4)$$

where $\alpha_1 = \mu_1\sqrt{\omega_{p_1}/2\varepsilon_0\hbar}$ and $\alpha_2 = \mu_2\sqrt{\omega_{p_2}/2\varepsilon_0\hbar}$ denote the coupling strength of the probe beams with the atoms, while μ_1 and μ_2 represent the dipole moments for the corresponding atomic transitions.

It should be noted that the diffraction terms containing the transverse derivatives $(2k_{p_1})^{-1}\nabla_{\perp}^2\mathcal{P}_1$ and $(2k_{p_2})^{-1}\nabla_{\perp}^2\mathcal{P}_2$ have been disregarded in the Maxwell equations (3) and (4), where $k_{p_1} = \omega_{p_1}/c$ and $k_{p_2} = \omega_{p_2}/c$ are the central wave vectors of the probe beams. One can evaluate these terms as $\nabla_{\perp}^2\mathcal{P}_{1,2} \sim w^{-2}\mathcal{P}_{1,2}$, where w represents a characteristic transverse dimension of the laser beams. It corresponds to the width of the vortex core if the beam carries an optical vortex or a characteristic width of a nonvortex beam. The change of the phase of the probe beams due to the diffraction term after passing the medium is then estimated to be $L/2kw^2$, where L is the length of the atomic cloud, with $k \approx k_{p_{1,2}}$. One can neglect the phase change $L/2kw^2$ when the sample length L is not too large, $L\lambda/w^2 \ll \pi$, where $\lambda = 2\pi/k$ is an optical wavelength [23,59,60]. For instance, by taking the length of the atomic cloud $L = 100 \mu\text{m}$, the characteristic transverse dimension of the beams $w = 20 \mu\text{m}$, and the wavelength $\lambda = 1 \mu\text{m}$, one obtains $L\lambda/w^2 = 0.25$. In that case the diffraction terms do not play an important role and can be safely dropped out, leading to Eqs. (3) and (4).

Assuming that the strength of the coupling of the probe fields with the atoms is the same $\alpha_1 = \alpha_2 = \alpha$, one arrives at the following equations for the slowly varying atomic amplitudes:

$$i\partial_t\Phi_{U_1} = \delta_{1f}\Phi_{U_1} - \alpha\mathcal{P}_1\Phi_Y - \mathcal{E}_{c_1}(r)e^{i\varphi}\Phi_R, \quad (5)$$

$$i\partial_t\Phi_{U_2} = \delta_{1f}\Phi_{U_2} - \alpha\mathcal{P}_2\Phi_Y - \mathcal{E}_{c_2}(r)e^{i2\varphi}\Phi_R, \quad (6)$$

$$i\partial_t\Phi_Y = (\delta_{2f} - i\Gamma)\Phi_Y - \alpha\mathcal{P}_1^*\Phi_{U_1} - \alpha\mathcal{P}_2^*\Phi_{U_2}, \quad (7)$$

where $\delta_{1f} = \omega_{U_1} - \omega_R - \omega_{c_1} = \omega_{U_2} - \omega_R - \omega_{c_2}$ describes the one-photon detuning, $\delta_{2f} = \omega_{p_1} - \omega_{c_1} + \omega_Y - \omega_R = \omega_{p_2} - \omega_{c_2} + \omega_Y - \omega_R$ represents the two-photon detuning, and Γ is the decay rate of the level Y . Here, ω_{U_1} , ω_{U_2} , and ω_Y are energies of the atomic states U_1 , U_2 , and Y , respectively.

We consider the case of monochromatic probe beams with the time-independent amplitudes \mathcal{P}_1 and \mathcal{P}_2 and the spatially homogeneous atomic amplitudes Φ_R , Φ_Y , Φ_{U_1} , and Φ_{U_2} . We will look for the stationary solutions characterized by the time-independent atomic amplitudes Φ_R , Φ_Y , Φ_{U_1} , and Φ_{U_2} , giving

$$c\partial_z\mathcal{P}_1 - i\alpha\Phi_Y^*\Phi_{U_1} = 0, \quad (8)$$

$$c\partial_z\mathcal{P}_2 - i\alpha\Phi_Y^*\Phi_{U_2} = 0, \quad (9)$$

$$\delta_{1f}\Phi_{U_1} - \alpha\mathcal{P}_1\Phi_Y - \mathcal{E}_{c_1}(r)e^{i l_1\varphi}\Phi_R = 0, \quad (10)$$

$$\delta_{1f}\Phi_{U_2} - \alpha\mathcal{P}_2\Phi_Y - \mathcal{E}_{c_2}(r)e^{i l_2\varphi}\Phi_R = 0, \quad (11)$$

$$(\delta_{2f} - i\Gamma)\Phi_Y - \alpha\mathcal{P}_1^*\Phi_{U_1} - \alpha\mathcal{P}_2^*\Phi_{U_2} = 0. \quad (12)$$

The pump waves are far detuned from the electronic excited levels, i.e., we take that $\delta_{1f} \gg |\Omega_{c_j}|$. In this case, the pump fields do not cause noticeable depletion of the ground state [73]. Specifically, for the parameters used below for the calculations the depletion is lower than 1%. Also, for a large one-photon detuning δ_{1f} ($\delta_{1f}|\delta_{2f} - i\gamma| \gg \alpha^2|\mathcal{P}_{1,2}|^2$), Eqs. (10) and (11) give

$$\Phi_{U_1} = \frac{\mathcal{E}_{c_1}(r)}{\delta_{1f}}e^{i l_1\varphi}\Phi_R, \quad (13)$$

$$\Phi_{U_2} = \frac{\mathcal{E}_{c_2}(r)}{\delta_{1f}}e^{i l_2\varphi}\Phi_R. \quad (14)$$

Substituting Eqs. (13) and (14) into Eq. (12) yields

$$\Phi_Y = \frac{\alpha\Phi_R}{\delta_{1f}(\delta_{2f} - i\Gamma)}[\mathcal{E}_{c_1}(r)e^{i l_1\varphi}\mathcal{P}_1^* + \mathcal{E}_{c_2}(r)e^{i l_2\varphi}\mathcal{P}_2^*]. \quad (15)$$

Using Eqs. (13)–(15) the propagation equations for both probe fields P_1 and P_2 [Eqs. (8) and (9)] take the form

$$\partial_z P_1 - i\beta \left(\frac{|\mathcal{E}_{c_1}(r)|^2 \mathcal{P}_1 + \mathcal{E}_{c_1}(r)\mathcal{E}_{c_2}^*(r)e^{i(l_1-l_2)\varphi}\mathcal{P}_2}{(\delta_{2f} + i\Gamma)} \right) = 0, \quad (16)$$

$$\partial_z P_2 - i\beta \left(\frac{\mathcal{E}_{c_1}^*(r)\mathcal{E}_{c_2}(r)e^{i(l_2-l_1)\varphi}\mathcal{P}_1 + |\mathcal{E}_{c_2}(r)|^2 \mathcal{P}_2}{(\delta_{2f} + i\Gamma)} \right) = 0, \quad (17)$$

with

$$\beta = \frac{\alpha^2|\Phi_R|^2}{c\delta_{1f}^2} = \frac{\alpha^2 n}{c\delta_{1f}^2}. \quad (18)$$

We now introduce new fields representing superpositions of the original probe beams

$$\psi = \frac{1}{\mathcal{E}_c(r)}[\mathcal{E}_{c_1}^*(r)e^{-i l_1\varphi}\mathcal{P}_1 + \mathcal{E}_{c_2}^*(r)e^{-i l_2\varphi}\mathcal{P}_2], \quad (19)$$

$$\xi = \frac{1}{\mathcal{E}_c(r)}[\mathcal{E}_{c_2}(r)e^{i l_2\varphi}\mathcal{P}_1 - \mathcal{E}_{c_1}(r)e^{i l_1\varphi}\mathcal{P}_2], \quad (20)$$

where

$$\mathcal{E}_c(r) = \sqrt{|\mathcal{E}_{c_1}(r)|^2 + |\mathcal{E}_{c_2}(r)|^2} \quad (21)$$

is the total strength of the control fields. Calling on Eqs. (19) and (20), one can rewrite Eqs. (16) and (17) as

$$\partial_z \psi - i\kappa \psi = 0, \quad (22)$$

$$\partial_z \xi = 0, \quad (23)$$

where

$$\kappa = \beta \frac{\mathcal{E}_c^2(r)}{(\delta_{2f} + i\Gamma)}. \quad (24)$$

This behavior of the modes ψ and ξ is similar to propagation in the double-lambda system. Equations (22) and (23) clearly

show that one of the superposition fields ψ interacts with the atoms, while another field ξ does not interact and propagates as in the free space. The solution of Eq. (22) reads

$$\psi(z) = \frac{1}{\mathcal{E}_c(r)}[\mathcal{E}_{c_1}^*(r)e^{-i l_1\varphi}\mathcal{P}_1(0) + \mathcal{E}_{c_2}^*(r)e^{-i l_2\varphi}\mathcal{P}_2(0)] \times e^{i\frac{\Gamma}{\delta_{1f}^2}\frac{\mathcal{E}_c^2(r)}{(\delta_{2f}+i\Gamma)}\frac{z}{L_\Gamma}}, \quad (25)$$

where

$$L_\Gamma = \frac{\Gamma c}{n\alpha^2} \quad (26)$$

determines the characteristic length related to the decay of the excited level Y .

The group velocity of the light given by Eq. (25) can be calculated as

$$v_g = \frac{c}{1 + \frac{\alpha^2 n \mathcal{E}_c^2(r)}{\delta_{1f}^2} \frac{\Gamma^2 - \delta_{2f}^2}{(\delta_{2f}^2 + \Gamma^2)^2}}. \quad (27)$$

Equation (27) is very similar to group velocity in a Raman system with a single probe beam. Clearly, when $\Gamma < \delta_{2f}$ the group velocity exceeds c providing the superluminality. On the other hand, the slow light propagates in the medium when $\Gamma > \delta_{2f}$ ($v_g < c$). In particular, the superluminal propagation is associated with the amplification since the energy of pump fields is transferred to the probe fields. This can be easily seen from the fact that the coefficient κ in Eq. (24) is a complex number.

In the following we consider a case where the first pump field Ω_{c_1} is a vortex $l_1 \neq 0$, while the second pump field is a nonvortex Gaussian beam with $l_2 = 0$. We have made such an assumption to avoid the zero denominator when $r \rightarrow 0$ in Eq. (25) if $l_2 \neq 0$. Numerical simulations presented in Figs. 2–7 show the superposition beam given by Eq. (25) in a transverse plane of the beam at $z = L_\Gamma$.

Figure 2 (4) displays the numerical results of the intensity distributions of the superposition beam ψ when the two-photon detuning is larger (smaller) than Γ corresponding to superluminal (subluminal) propagation of superposition pulse inside the medium, and for different vorticities $l_1 = 1-6$. Figure 3 (5) shows the corresponding helical phase patterns. For simulations we have selected $\delta_{2f} = 4\Gamma$ and $\delta_{2f} = 0$ corresponding to the superluminal and subluminal situations, respectively.

The resulting beam is seen to have a very particular shape. The center of the superposition beam contains no vortex and is surrounded by l_1 singly charged peripheral vortices of sign $l_1/|l_1|$. The peripheral vortices are distributed at angles

$$\varphi_p = \frac{n\pi}{l_1}, \quad (28)$$

with an approximate radial distance to the beam center

$$r_p \approx \left(|l_1|! \frac{|\Omega_{c_2}|}{|\Omega_{c_1}|} \right)^{\frac{1}{2|l_1|}}, \quad (29)$$

where $n = 1 \dots 2|l_1|$ is an integer for each peripheral vortex [68]. The off-axis vortices are placed at the same radial distance from the core of the superposition beam.

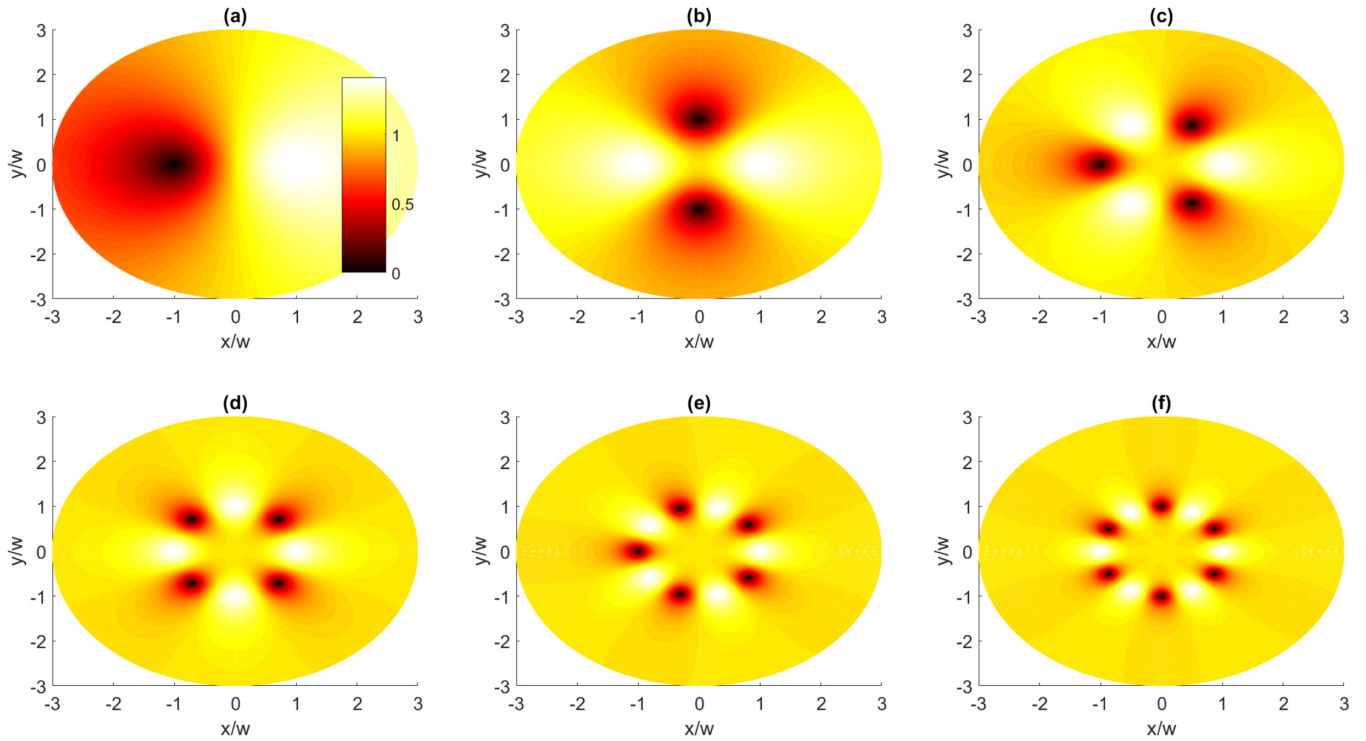


FIG. 2. Intensity distributions (in arbitrary units) of the superluminal superposition beam ψ featured in Eq. (25) with different vorticities $l_1 = 1-6$ (a)–(e). Here the parameters are $|\Omega_{c_1}| = |\Omega_{c_2}| = \Gamma$, $\delta_{1f} = 30\Gamma$, $z = L_\Gamma$, $l_2 = 0$, and $\delta_{2f} = 4\Gamma$.

Such images of the subluminal or superluminal vortices appear as two initial pump beams with different azimuthal indices $l_1 \neq 0$ and $l_2 = 0$ superimposed leading to formation of the off-center vortices with shifted axes. To elucidate this better, let us consider Fig. 3(f), which is plotted for $l_1 = 6$.

Note that we have considered a case where the strength of both coupling beams are the same ($|\Omega_{c_1}| = |\Omega_{c_2}| = \Gamma$). Region A is dominated by the vortex beam with Ω_{c_1} and $l_1 = 6$, while the inner region B is dominated by the Gaussian beam Ω_{c_2} with $l_2 = 0$. The peripheral vortices are located precisely at

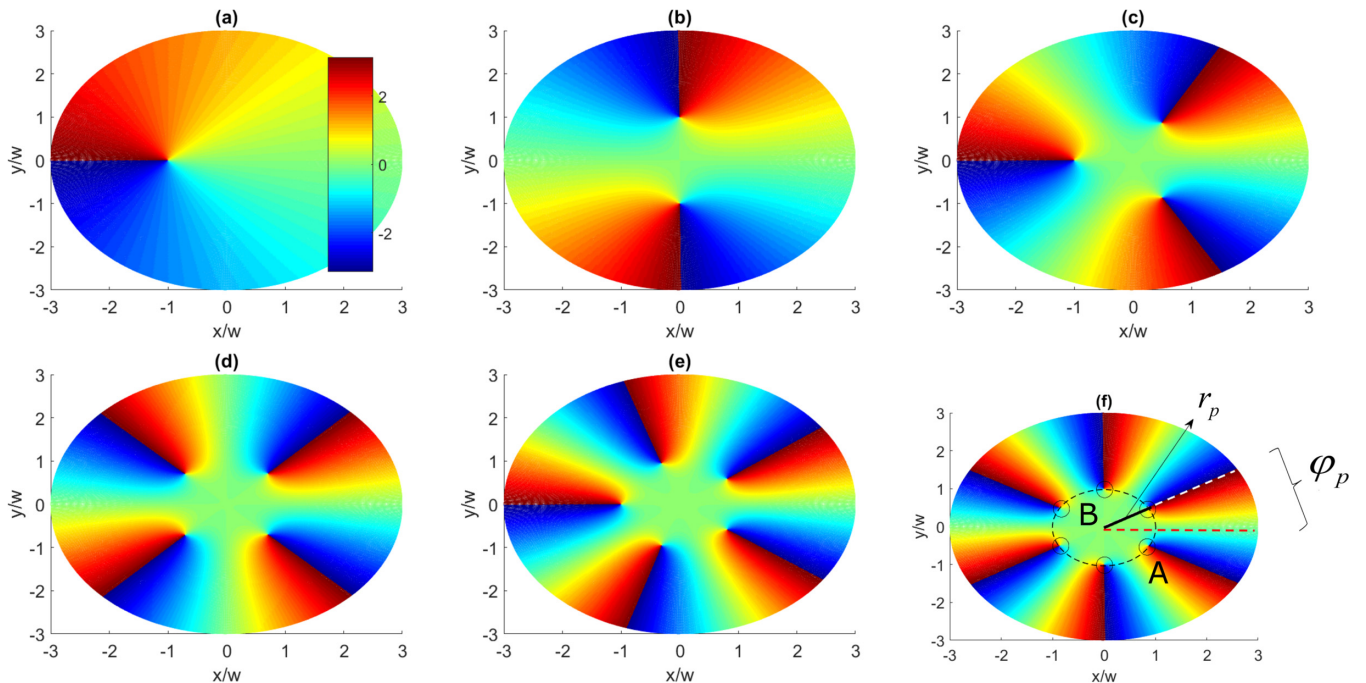


FIG. 3. Helical phase patterns of the superluminal superposition beam ψ featured in Eq. (25) with different vorticities $l_1 = 1-6$ (a)–(e). The parameters are taken to be the same as in Fig. 2.

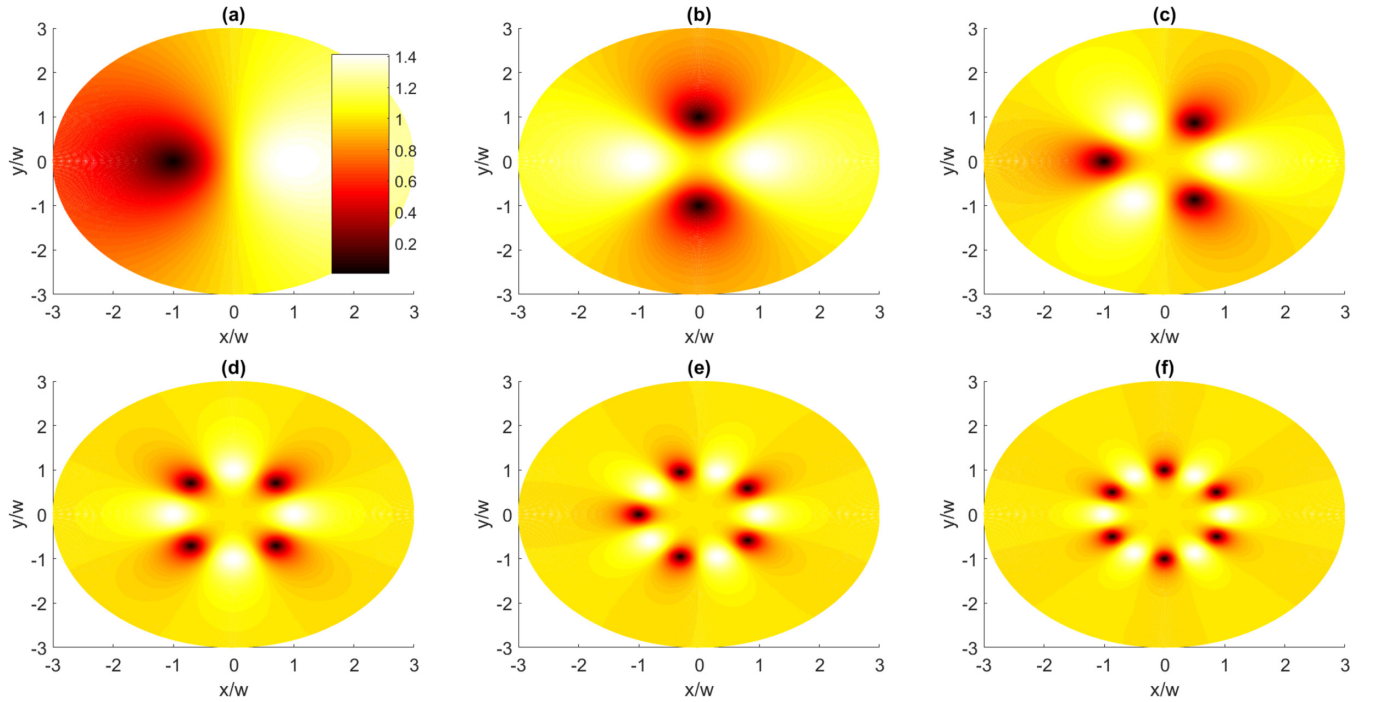


FIG. 4. Intensity distributions (in arbitrary units) of the subluminal superposition beam ψ featured in Eq. (25) with different vorticities $l_1 = 1-6$ (a)–(e). Here the parameters are $|\Omega_{c1}| = |\Omega_{c2}| = \Gamma$, $\delta_{1f} = 30\Gamma$, $z = L_\Gamma$, and $\delta_{2f} = 0$.

the boundary between the two regions, which is a circle of the radius r_p .

Comparing Figs. 3 and 5 shows that the phase structures of the superluminal and subluminal beams look similar for smaller OAM numbers. Yet, the phase patterns of a superluminal superposition beam are bent with respect to the subluminal

one when the topological charge l_1 increases, as one can see comparing Figs. 6(a)–6(d) with 6(e)–6(h). In fact, the exponent of the factor $e^{i\frac{\Gamma}{\delta_{1f}} \frac{\mathcal{E}_c^2(r)}{(\delta_{2f} + i\Gamma)} \frac{z}{L_\Gamma}}$ in Eq. (25) contains the term $\mathcal{E}_c^2(r)$, which is not uniform in the (x, y) plane, resulting in bending of the phase patterns when δ_{2f} is nonzero.

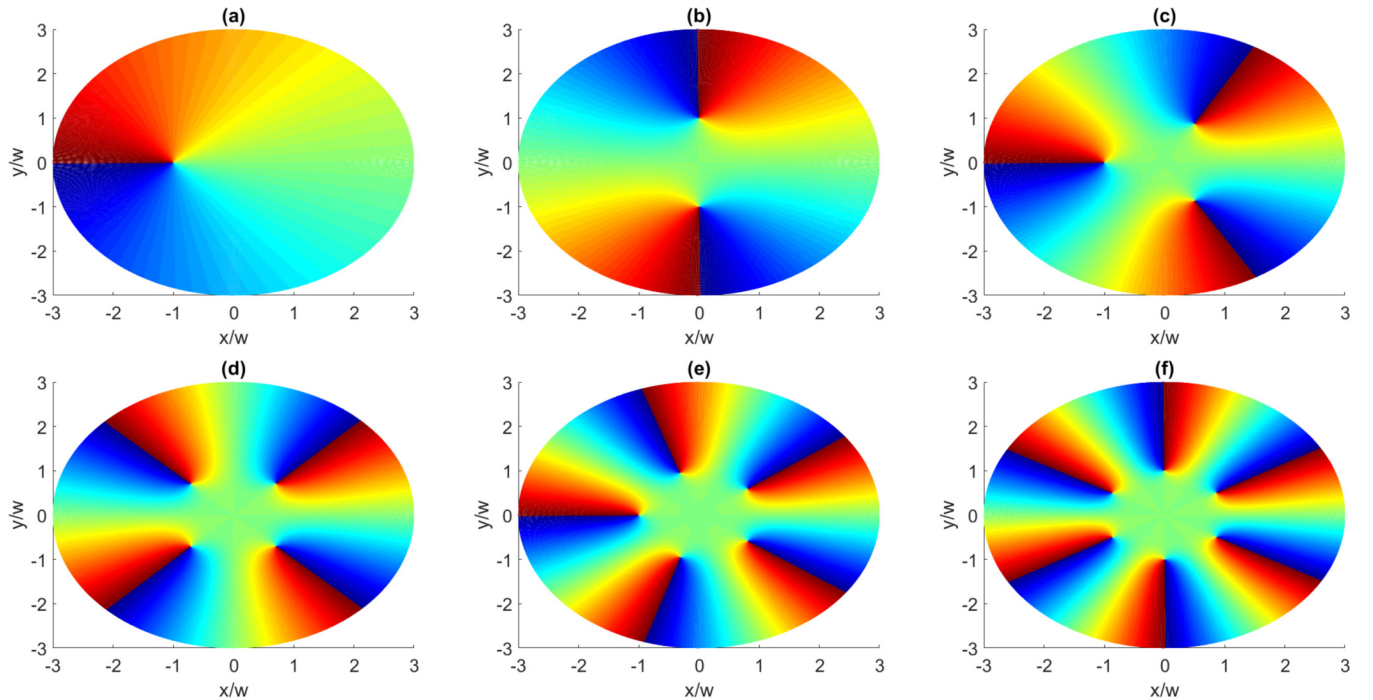


FIG. 5. Helical phase patterns of the subluminal superposition beam ψ featured in Eq. (25) with different vorticities $l_1 = 1-6$ (a)–(e). The parameters are the same as Fig. 4.

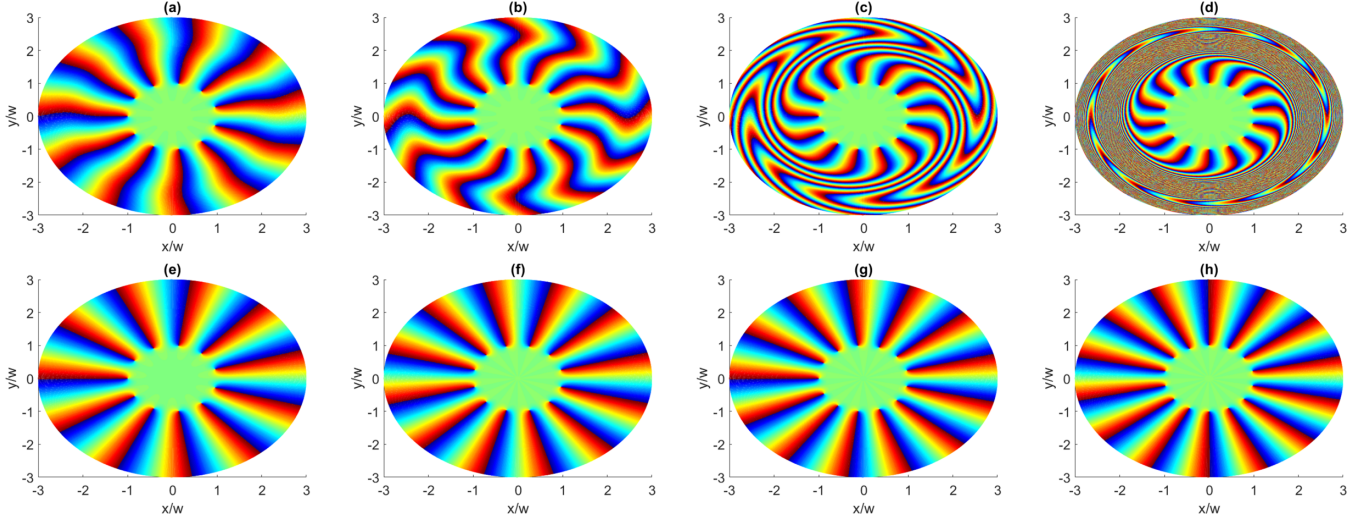


FIG. 6. Helical phase patterns of the superposition beam ψ featured in Eq. (25) with different vorticities $l_1 = 11$ (a), (e), $l_1 = 12$ (b), (f), $l_1 = 13$ (c), (g), and $l_1 = 14$ (d), (h). Here $\delta_{2f} = 4\Gamma$ (a), (b), (c), (d), $\delta_{2f} = 0$ (e), (f), (g), (h), and the other parameters are the same as in Fig. 2.

Figure 7 illustrates the effect of the strength of pump beams $|\Omega_{c_1}|$ and $|\Omega_{c_2}|$ on intensity distributions and the corresponding helical phase patterns. We plot only the case of the superluminality ($\delta_{2f} = 4\Gamma$), as the results are very similar to the subluminal case. It is apparent from Figs. 7(a) and 7(b) that the peripheral vortex shifts toward the center of the beam when $|\Omega_{c_1}| > |\Omega_{c_2}|$, while it moves away from the core when $|\Omega_{c_1}| < |\Omega_{c_2}|$ [see Figs. 7(c) and 7(d)]. As can be seen from Eq. (29), when $|\Omega_{c_1}| > |\Omega_{c_2}|$ ($|\Omega_{c_1}| < |\Omega_{c_2}|$), the radius r_p reduces (increases) and the position of the peripheral vortex moves radially in (out).

A. Exchange of optical vortices

We will now assume that only one probe field \mathcal{P}_1 is initially incident on the atomic cloud $z = 0$ [$\mathcal{P}_1(0) = \mathcal{P}$]. The amplitude of the second probe field is zero at the beginning [$\mathcal{P}_2(0) = 0$]. In this case, Eqs. (19) and (20) reduce to

$$\psi(0) = \frac{1}{\mathcal{E}_c(r)} [\mathcal{E}_{c_1}^*(r) e^{-il_1\varphi} \mathcal{P}], \quad (30)$$

$$\xi(0) = \frac{1}{\mathcal{E}_c(r)} [\mathcal{E}_{c_2}(r) e^{il_2\varphi} \mathcal{P}]. \quad (31)$$

The electric fields of the probe beams inside the atomic cloud can be obtained from the fields ψ and ξ as

$$\begin{aligned} \mathcal{P}_1(z) &= \frac{1}{\mathcal{E}_c(r)} [\mathcal{E}_{c_1}(r) e^{il_1\varphi} \psi(z) + \mathcal{E}_{c_2}^*(r) e^{-il_2\varphi} \xi(z)] \\ &= \left(1 + \frac{\mathcal{E}_{c_1}^2(r)}{\mathcal{E}_c^2(r)} (e^{i\kappa z} - 1) \right) \mathcal{P}, \end{aligned} \quad (32)$$

$$\begin{aligned} \mathcal{P}_2(z) &= \frac{1}{\mathcal{E}_c(r)} [\mathcal{E}_{c_2}(r) e^{il_2\varphi} \psi(z) - \mathcal{E}_{c_1}^*(r) e^{-il_1\varphi} \xi(z)] \\ &= \frac{\mathcal{E}_{c_2}(r) \mathcal{E}_{c_1}^*(r)}{\mathcal{E}_c^2(r)} e^{i(l_2 - l_1)\varphi} (e^{i\kappa z} - 1) \mathcal{P}, \end{aligned} \quad (33)$$

where κ is given by Eq. (24). The intensity distributions and the corresponding helical phase pattern of the generated second probe vortex beam are shown in Fig. 8 for $\delta_{2f} = 4\Gamma$ and different topological charge numbers. A doughnut intensity profile is observed with a dark hollow in the center. The phase jumps from zero to $n\pi$ around the singularity point. As Eq. (33) shows, the generated field contains a phase factor of $e^{i(l_2 - l_1)\varphi}$. If the first pump field is a vortex but the second one is a nonvortex beam, the generated probe field acquires a vortex of charge $-l_1$. On the other hand, if only the second

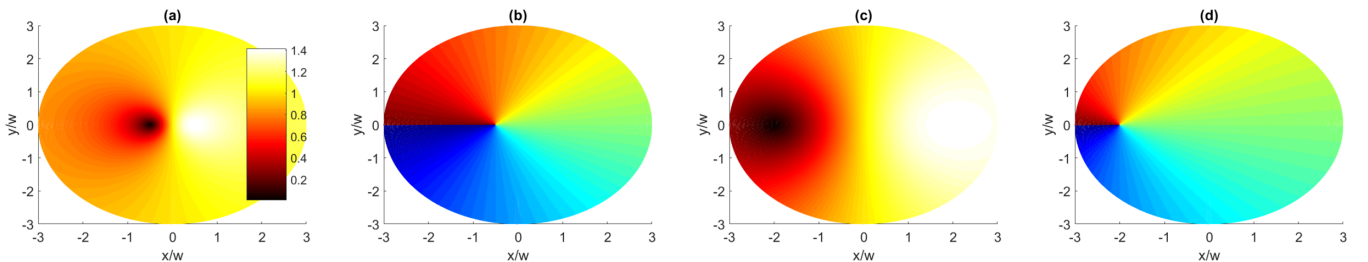


FIG. 7. Intensity distributions (a), (c) in arbitrary units as well as the corresponding helical phase patterns (b), (d) of the superposition beam ψ featured in Eq. (25). Here $|\Omega_{c_1}| = \Gamma$, $|\Omega_{c_2}| = 0.5\Gamma$ (a), (b) and $|\Omega_{c_1}| = 0.5\Gamma$, $|\Omega_{c_2}| = \Gamma$ (c), (d); $l_1 = 1$ and the other parameters are the same as in Fig. 2.

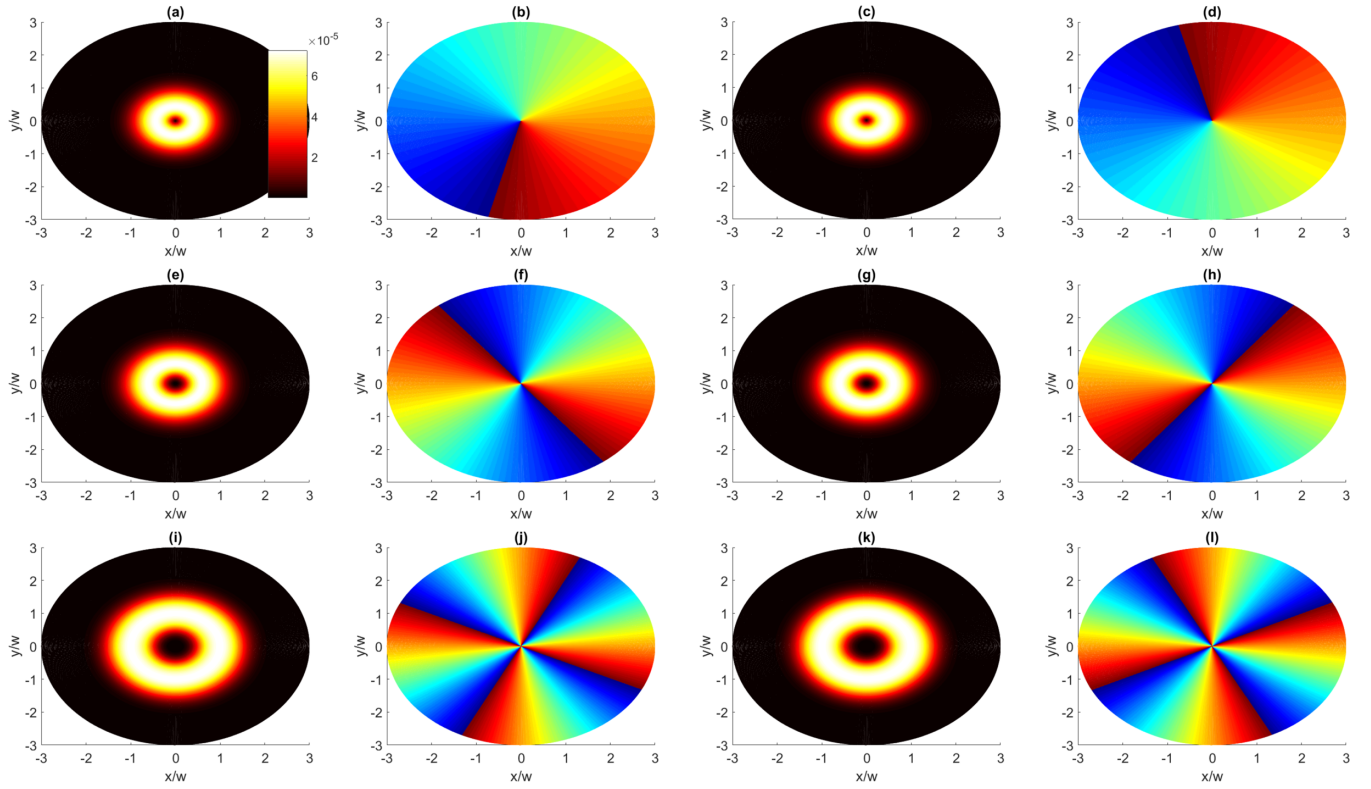


FIG. 8. Intensity distributions (a), (c), (e), (g), (i), (k) in arbitrary units as well as the corresponding helical phase patterns (b), (d), (f), (h), (j), (l) of the generated second probe vortex beam \mathcal{P}_2 featured in Eq. (33) when $l_1 = 1, l_2 = 0$ (a), (b), $l_1 = 0, l_2 = 1$ (c), (d), $l_1 = 2, l_2 = 0$ (e), (f), $l_1 = 0, l_2 = 2$ (g), (h), $l_1 = 4, l_2 = 0$ (i), (j), and $l_1 = 0, l_2 = 4$ (k), (l). Here $\delta_{2f} = 4\Gamma$ and the other parameters are the same as Fig. 2.

pump beam is a vortex with the charge l_2 , the generated probe beam has a vorticity l_2 .

B. Influence of phase mismatch

Thus far we have ignored a small phase mismatch between the four waves described by

$$\Delta_k = (\mathbf{k}_{p_1} - \mathbf{k}_{c_1} + \mathbf{k}_{c_2} - \mathbf{k}_{p_2}) \cdot \hat{\mathbf{e}}_z, \quad (34)$$

where $\hat{\mathbf{e}}_z$ is the unit vector along the z axis and \mathbf{k}_{p_1} , \mathbf{k}_{p_2} , \mathbf{k}_{c_1} , and \mathbf{k}_{c_2} are the wave vectors of the control and probe beams. We consider the situation when all the light beams co-propagate (almost) in the same direction. With the phase mismatch Δ_k included, the wave equations Eqs. (16) and (17) can be rewritten using Eqs. (1) and (2) [59]:

$$\partial_z \mathcal{P}_1 - ik \frac{\Omega_{c_1}}{\mathcal{E}_c^2} (\Omega_{c_1}^* \mathcal{P}_1 + \Omega_{c_2}^* \mathcal{P}_2) = 0, \quad (35)$$

$$\partial_z \mathcal{P}_2 + i\Delta_k \mathcal{P}_2 - ik \frac{\Omega_{c_2}}{\mathcal{E}_c^2} (\Omega_{c_1}^* \mathcal{P}_1 + \Omega_{c_2}^* \mathcal{P}_2) = 0. \quad (36)$$

Taking the derivative ∂_z of the superpositions (19) and (20) and using Eqs. (35) and (36) we get

$$\partial_z \psi - ik\psi + i\Delta_k \left(\frac{|\Omega_{c_2}|^2}{\mathcal{E}_c^2} \psi + \frac{\Omega_{c_1}^* \Omega_{c_2}^*}{\mathcal{E}_c^2} \xi \right) = 0, \quad (37)$$

$$\partial_z \xi + i\Delta_k \left(\frac{|\Omega_{c_1}|^2}{\mathcal{E}_c^2} \xi + \frac{\Omega_{c_1} \Omega_{c_2}}{\mathcal{E}_c^2} \psi \right) = 0. \quad (38)$$

In contrast to Eqs. (22) and (23), the propagation equations (37) and (38) are coupled due to the phase mismatch Δ_k . This means that ψ and ξ are not independent propagating modes. In principle, one needs to find the proper uncoupled propagating modes and calculate their dispersion and velocities. However, if Δ_k is sufficiently small, then those modes will differ only slightly from ψ and ξ . From Eq. (37) we can estimate the following condition when Δ_k can be considered to be small enough:

$$\Delta_k \ll |\kappa|. \quad (39)$$

Using Eqs. (1), (2), (21), and (24) and assuming that only the first pump field Ω_{c_1} is a vortex with $l_1 \neq 0$, while the second pump field is a nonvortex Gaussian beam with $l_2 = 0$, the requirement for the dimensionless quantity $\Delta_k L_\Gamma$ reads

$$\Delta_k L_\Gamma \ll \frac{\Gamma}{\delta_{1f}^2 (\sqrt{\delta_{2f}^2 + \Gamma^2})} \times (|\Omega_{c_1}|^2 (r/w)^{2|l_1|} e^{-2r^2/w^2} + |\Omega_{c_2}|^2), \quad (40)$$

which for the position r for which Ω is smallest, and for $|\Omega_{c_2}| = \Gamma$, $\delta_{1f} = \Gamma$, and $\delta_{2f} = 0$, it reduces to $\Delta_k L_\Gamma \ll 1$.

III. DOUBLE RAMAN DOUBLET SCHEME

In this section we present a more favorable scenario for the generation of off-axis vortices. We consider a situation where four strong pump beams act on the atomic ensemble (Fig. 9).

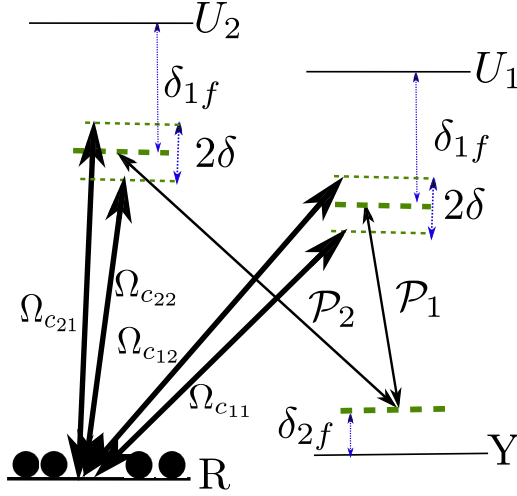


FIG. 9. Schematic diagram of the double-Raman doublet scheme.

This situation corresponds to a Raman doublet for each of the probe beams.

We assume four-photon resonances $\omega_{c_{11}} - \omega_{p_1} = \omega_{c_{21}} - \omega_{p_2}$ and $\omega_{c_{12}} - \omega_{p_1} = \omega_{c_{22}} - \omega_{p_2}$, where $\omega_{c_{11}}$, $\omega_{c_{12}}$, $\omega_{c_{21}}$, and $\omega_{c_{22}}$ are frequencies of the pump beams. To describe the propagation of the probe beams in the medium, we

separate the atomic amplitudes into two parts oscillating with different frequencies: $\Psi_Y = \Psi_{Y_1} + \Psi_{Y_2}$, $\Psi_{U_1} = \Psi_{U_{11}} + \Psi_{U_{12}}$, and $\Psi_{U_2} = \Psi_{U_{21}} + \Psi_{U_{22}}$. Recalling the slowly changing amplitudes and neglecting the terms oscillating with a large frequency $2\delta = \omega_{c_{12}} - \omega_{c_{11}} = \omega_{c_{22}} - \omega_{c_{21}}$, the equations for the matter fields read

$$c\partial_z P_1 = i\alpha\Phi_{Y_1}^* \frac{\mathcal{E}_{c_{11}}(r)}{\delta_{1f}} e^{i l_{11}\varphi} \Phi_R + i\alpha\Phi_{Y_2}^* \frac{\mathcal{E}_{c_{12}}(r)}{\delta_{1f}} e^{i l_{12}\varphi} \Phi_R, \quad (41)$$

$$c\partial_z P_2 = i\alpha\Phi_{Y_1}^* \frac{\mathcal{E}_{c_{21}}(r)}{\delta_{1f}} e^{i l_{21}\varphi} \Phi_R + i\alpha\Phi_{Y_2}^* \frac{\mathcal{E}_{c_{22}}(r)}{\delta_{1f}} e^{i l_{22}\varphi} \Phi_R, \quad (42)$$

$$\Phi_{Y_1} = \frac{\alpha\Phi_R}{(\delta_{2f} + \delta - i\Gamma)\delta_{1f}} [\mathcal{E}_{c_{11}}(r)e^{i l_{11}\varphi} \mathcal{P}_1^* + \mathcal{E}_{c_{21}}(r)e^{i l_{21}\varphi} \mathcal{P}_2^*], \quad (43)$$

$$\Phi_{Y_2} = \frac{\alpha\Phi_R}{(\delta_{2f} - \delta - i\Gamma)\delta_{1f}} [\mathcal{E}_{c_{12}}(r)e^{i l_{12}\varphi} \mathcal{P}_1^* + \mathcal{E}_{c_{22}}(r)e^{i l_{22}\varphi} \mathcal{P}_2^*], \quad (44)$$

where $\delta_{1f} = \omega_{U_1} - \omega_R - \frac{1}{2}(\omega_{c_{11}} + \omega_{c_{12}}) = \omega_{U_2} - \omega_R - \frac{1}{2}(\omega_{c_{21}} + \omega_{c_{22}})$ is an average one-photon detuning and $\delta_{2f} = \omega_{p_1} + \omega_Y - \omega_R - \frac{1}{2}(\omega_{c_{11}} + \omega_{c_{12}}) = \omega_{p_2} + \omega_Y - \omega_R - \frac{1}{2}(\omega_{c_{21}} + \omega_{c_{22}})$ denotes an average two-photon detuning. Equations (41)–(44) give the following equations for the propagation of the probe fields:

$$\partial_z P_1 - i\beta \left(\frac{|\mathcal{E}_{c_{11}}(r)|^2 P_1 + \mathcal{E}_{c_{11}}(r)\mathcal{E}_{c_{21}}^*(r)e^{i(l_{11}-l_{21})\varphi} P_2}{\delta_{2f} + \delta + i\Gamma} + \frac{|\mathcal{E}_{c_{12}}(r)|^2 P_1 + \mathcal{E}_{c_{12}}(r)\mathcal{E}_{c_{22}}^*(r)e^{i(l_{12}-l_{22})\varphi} P_2}{\delta_{2f} - \delta + i\Gamma} \right) = 0, \quad (45)$$

$$\partial_z P_2 - i\beta \left(\frac{\mathcal{E}_{c_{21}}(r)\mathcal{E}_{c_{11}}^*(r)e^{i(l_{21}-l_{11})\varphi} P_1 + |\mathcal{E}_{c_{21}}(r)|^2 P_2}{\delta_{2f} + \delta + i\Gamma} + \frac{\mathcal{E}_{c_{22}}(r)\mathcal{E}_{c_{12}}^*(r)e^{i(l_{22}-l_{12})\varphi} P_1 + |\mathcal{E}_{c_{22}}(r)|^2 P_2}{\delta_{2f} - \delta + i\Gamma} \right) = 0. \quad (46)$$

We consider a particular situation in which

$$\frac{\mathcal{E}_{c_{12}}(r)}{\mathcal{E}_{c_{11}}(r)} e^{i(l_{12}-l_{11})\varphi} = \frac{\mathcal{E}_{c_{22}}(r)}{\mathcal{E}_{c_{21}}(r)} e^{i(l_{22}-l_{21})\varphi}. \quad (47)$$

Defining the generalized quantities

$$\mathcal{E}_{c_1}(r) = \sqrt{|\mathcal{E}_{c_{11}}(r)|^2 + |\mathcal{E}_{c_{21}}(r)|^2}, \quad (48)$$

$$\mathcal{E}_{c_2}(r) = \sqrt{|\mathcal{E}_{c_{12}}(r)|^2 + |\mathcal{E}_{c_{22}}(r)|^2}, \quad (49)$$

and introducing new fields representing superpositions of the original probe fields

$$\psi = \frac{1}{\mathcal{E}_{c_1}(r)} [\mathcal{E}_{c_{11}}^*(r)e^{-i l_{11}\varphi} \mathcal{P}_1 + \mathcal{E}_{c_{21}}^*(r)e^{-i l_{21}\varphi} \mathcal{P}_2], \quad (50)$$

$$\xi = \frac{1}{\mathcal{E}_{c_1}(r)} [\mathcal{E}_{c_{21}}(r)e^{i l_{21}\varphi} \mathcal{P}_1 - \mathcal{E}_{c_{11}}(r)e^{i l_{11}\varphi} \mathcal{P}_2], \quad (51)$$

we reduce Eqs. (45) and (46) to Eqs. (22) and (23) with

$$\kappa = \beta \left(\frac{\mathcal{E}_{c_1}^2(r)}{(\delta_{2f} + \delta + i\Gamma)} + \frac{\mathcal{E}_{c_2}^2(r)}{(\delta_{2f} - \delta + i\Gamma)} \right). \quad (52)$$

Again, the field ξ does not interact and propagates as in free space, while the new field ψ interacts with the atoms.

Assuming

$$\mathcal{E}_{c_1}(r) = \mathcal{E}_{c_2}(r) = \mathcal{E}_c(r), \quad (53)$$

and $\delta_{2f} = 0$, one finds

$$v_g = \frac{c}{1 + \frac{2\alpha^2 n \mathcal{E}_c^2(r)}{\delta_{1f}^2} \frac{\Gamma^2 - \delta^2}{(\delta^2 + \Gamma^2)^2}}. \quad (54)$$

Thus for $\delta > \Gamma$ ($\delta < \Gamma$) the group velocity is larger (smaller) than c providing superluminal (subluminal) propagation. In addition, according to Eq. (52), the generated fast light experiences amplification again. We see that, in contrast to the double-Raman scheme, we have sup- or superluminal propagation even for zero two-photon detuning $\delta_{2f} = 0$. In order to have off-axis optical vortices satisfying Eqs. (47), (48), (49), and (53) and to avoid zero denominator at the core in $\psi(z) = \psi(0)e^{ikz}$, we can consider $l_{11} = -l_{22} = l \neq 0$ (i.e., $\Omega_{c_{11}}$ and $\Omega_{c_{22}}$ are vortices) but $l_{21} = l_{12} = 0$ (i.e., $\Omega_{c_{11}}$ and $\Omega_{c_{22}}$ are nonvortex Gaussian beams).

Let us assume that only one probe field \mathcal{P}_1 is incident on the atomic cloud [$\mathcal{P}_1(0) = \mathcal{P}$]. The amplitude of the second

probe field at the beginning of the atomic cloud $z = 0$ is zero [$\mathcal{P}_2(0) = 0$]. In this case, Eqs. (50) and (51) reduce to

$$\psi(0) = \frac{\mathcal{E}_{c11}^*(r)e^{-il\varphi}}{\mathcal{E}_{c1}(r)}\mathcal{P}, \quad (55)$$

$$\xi(0) = \frac{\mathcal{E}_{c21}(r)}{\mathcal{E}_{c1}(r)}\mathcal{P}. \quad (56)$$

The electric fields of the probe beams inside the atomic cloud can be obtained from the fields ψ and ξ as

$$\mathcal{P}_1(z) = \left(1 + \frac{\mathcal{E}_{c11}^2(r)}{\mathcal{E}_c^2(r)}(e^{i\kappa z} - 1)\right)\mathcal{P}, \quad (57)$$

$$\mathcal{P}_2(z) = \frac{\mathcal{E}_{c21}(r)\mathcal{E}_{c11}^*(r)}{\mathcal{E}_c^2(r)}e^{-il\varphi}(e^{i\kappa z} - 1)\mathcal{P}, \quad (58)$$

with κ featured in Eq. (52). Exchange of optical vortices with opposite vorticity is now possible between the pump field Ω_{c11} and the generated probe field \mathcal{P}_2 even for zero two-photon detuning $\delta_{2f} = 0$.

IV. SUMMARY

We have investigated the formation of off-axis vortices with shifted axes in a double-Raman gain medium interacting with two weak probe fields as well as two stronger pump lasers which can contain an optical vortex. In such a medium

only a particular superposition of the probe fields is coupled with the atoms, while an orthogonal combination of the probe fields does not interact with the atoms and propagates as in the free space. Assuming that one of the pump fields is a vortex, depending on the two-photon detuning, the superposition off-axis vortex beam can propagate either with the slow or the fast group velocity. One can control the position of the peripheral vortices by the vorticity and intensity of the pump fields. The model for creation of the off-center fast and slow light vortices can also be generalized to a more complicated double Raman doublet with four pump fields. A possible experimental realization of the proposed scheme for off-axis optical vortices can be implemented for an atomic cesium vapor cell at room temperature. All cesium atoms are to be prepared in the ground-state hyperfine magnetic sublevel $6S_{1/2}, |F = 4, m = -4\rangle$ serving as the level R in our scheme. The magnetic sublevel $6S_{1/2}, |F = 4, m = -2\rangle$ corresponds to the level Y . Also, the levels $5P_{3/2}, |F = 4, m = -3\rangle$ and $6P_{1/2}, |F = 4, m = -3\rangle$ are excited levels U_1 and U_2 , respectively [41].

ACKNOWLEDGMENTS

This research was funded by the European Social Fund under Grant No. 09.3.3-LMT-K-712-01-0051.

-
- [1] S. E. Harris, *Phys. Today* **50**, 36 (1997).
[2] M. Fleischhauer, A. Imamoglu, and J. P. Marangos, *Rev. Mod. Phys.* **77**, 633 (2005).
[3] E. Paspalakis, N. J. Kylstra, and P. L. Knight, *Phys. Rev. A* **65**, 053808 (2002).
[4] E. Paspalakis and Z. Kis, *J. Opt. B* **4**, S372 (2002).
[5] E. Paspalakis and Z. Kis, *Phys. Rev. A* **66**, 025802 (2002).
[6] J. Ruseckas, G. Juzeliūnas, P. Öhberg, and S. M. Barnett, *Phys. Rev. A* **76**, 053822 (2007).
[7] R. Grobe, F. T. Hioe, and J. H. Eberly, *Phys. Rev. Lett.* **73**, 3183 (1994).
[8] M. Fleischhauer and A. S. Manka, *Phys. Rev. A* **54**, 794 (1996).
[9] H. Wang, D. Goorskey, and M. Xiao, *Phys. Rev. Lett.* **87**, 073601 (2001).
[10] S. E. Harris, *Phys. Rev. Lett.* **72**, 52 (1994).
[11] E. Cerboneschi and E. Arimondo, *Phys. Rev. A* **52**, R1823 (1995).
[12] S. E. Harris, J. E. Field, and A. Imamoglu, *Phys. Rev. Lett.* **64**, 1107 (1990).
[13] L. Deng, M. G. Payne, and W. R. Garrett, *Phys. Rev. A* **58**, 707 (1998).
[14] H. Kang and Y. Zhu, *Phys. Rev. Lett.* **91**, 093601 (2003).
[15] H. R. Hamed and G. Juzeliūnas, *Phys. Rev. A* **91**, 053823 (2015).
[16] Y. Wu and L. Deng, *Phys. Rev. Lett.* **93**, 143904 (2004).
[17] Y. Wu and L. Deng, *Opt. Lett.* **29**, 2064 (2004).
[18] L. V. Hau, S. E. Harris, Z. Dutton, and C. H. Behroozi, *Nature (London)* **397**, 594 (1999).
[19] M. D. Lukin, *Rev. Mod. Phys.* **75**, 457 (2003).
[20] G. Juzeliūnas and P. Öhberg, *Phys. Rev. Lett.* **93**, 033602 (2004).
[21] J. Ruseckas, V. Kudriašov, G. Juzeliūnas, R. G. Unanyan, J. Otterbach, and M. Fleischhauer, *Phys. Rev. A* **83**, 063811 (2011).
[22] Q.-Q. Bao, X.-H. Zhang, J.-Y. Gao, Y. Zhang, C.-L. Cui, and J.-H. Wu, *Phys. Rev. A* **84**, 063812 (2011).
[23] J. Ruseckas, V. Kudriašov, I. A. Yu, and G. Juzeliūnas, *Phys. Rev. A* **87**, 053840 (2013).
[24] M.-J. Lee, J. Ruseckas, C.-Y. Lee, V. Kudriašov, K.-F. Chang, H.-W. Cho, G. Juzeliūnas, and I. A. Yu, *Nat. Commun.* **5**, 5542 (2014).
[25] D. F. Phillips, A. Fleischhauer, A. Mair, R. L. Walsworth, and M. D. Lukin, *Phys. Rev. Lett.* **86**, 783 (2001).
[26] C. Liu, Z. Dutton, C. H. Behroozi, and L. V. Hau, *Nature (London)* **409**, 490 (2001).
[27] M. D. Lukin and A. Imamoglu, *Nature (London)* **413**, 273 (2001).
[28] G. Juzeliūnas and H. J. Carmichael, *Phys. Rev. A* **65**, 021601(R) (2002).
[29] L. Ma, O. Slattery, and X. Tang, *J. Opt.* **19**, 043001 (2017).
[30] Y.-F. Hsiao, P.-J. Tsai, H.-S. Chen, S.-X. Lin, C.-C. Hung, C.-H. Lee, Y.-H. Chen, Y.-F. Chen, I. A. Yu, and Y.-C. Chen, *Phys. Rev. Lett.* **120**, 183602 (2018).
[31] K. J. Jiang, L. Deng, and M. G. Payne, *Phys. Rev. A* **76**, 033819 (2007).
[32] M. Mahmoudi, M. Sahrai, and H. Tajalli, *Phys. Lett. A* **357**, 66 (2006).
[33] S. qi Kuang, R. gang Wan, J. Kou, Y. Jiang, and J. yue Gao, *J. Opt. Soc. Am. B* **26**, 2256 (2009).
[34] A. M. Akulshin and R. J. McLean, *J. Opt.* **12**, 104001 (2010).
[35] S. Chu and S. Wong, *Phys. Rev. Lett.* **48**, 738 (1982).

- [36] A. M. Steinberg, P. G. Kwiat, and R. Y. Chiao, *Phys. Rev. Lett.* **71**, 708 (1993).
- [37] R. Y. Chiao, *Phys. Rev. A* **48**, R34 (1993).
- [38] A. Dogariu, A. Kuzmich, and L. J. Wang, *Phys. Rev. A* **63**, 053806 (2001).
- [39] R. T. Glasser, U. Vogl, and P. D. Lett, *Phys. Rev. Lett.* **108**, 173902 (2012).
- [40] P. Bianucci, C. R. Fietz, J. W. Robertson, G. Shvets, and C.-K. Shih, *Phys. Rev. A* **77**, 053816 (2008).
- [41] V. Kudriašov, J. Ruseckas, A. Mekys, A. Ekers, N. Bezuglov, and G. Juzeliūnas, *Phys. Rev. A* **90**, 033827 (2014).
- [42] L. Allen, M. J. Padgett, and M. Babiker, *Prog. Opt.* **39**, 291 (1999).
- [43] M. Padgett, J. Courtial, and L. Allen, *Phys. Today* **57**, 35 (2004).
- [44] M. Babiker, D. L. Andrews, and V. E. Lembessis, *J. Opt.* **21**, 013001 (2018).
- [45] M. Babiker, W. L. Power, and L. Allen, *Phys. Rev. Lett.* **73**, 1239 (1994).
- [46] G. Molina-Terriza, J. P. Torres, and L. Torner, *Phys. Rev. Lett.* **88**, 013601 (2001).
- [47] R. Pugatch, M. Shuker, O. Firstenberg, A. Ron, and N. Davidson, *Phys. Rev. Lett.* **98**, 203601 (2007).
- [48] Z. Dutton and J. Ruostekoski, *Phys. Rev. Lett.* **93**, 193602 (2004).
- [49] A. I. Bishop, T. A. Nieminen, N. R. Heckenberg, and H. Rubinsztein-Dunlop, *Phys. Rev. Lett.* **92**, 198104 (2004).
- [50] Q.-F. Chen, B.-S. Shi, Y.-S. Zhang, and G.-C. Guo, *Phys. Rev. A* **78**, 053810 (2008).
- [51] V. E. Lembessis and M. Babiker, *Phys. Rev. A* **82**, 051402(R) (2010).
- [52] J. Ruseckas, A. Mekys, and G. Juzeliūnas, *J. Opt.* **13**, 064013 (2011).
- [53] D.-S. Ding, Z.-Y. Zhou, B.-S. Shi, X.-B. Zou, and G.-C. Guo, *Opt. Lett.* **37**, 3270 (2012).
- [54] G. Walker, A. S. Arnold, and S. Franke-Arnold, *Phys. Rev. Lett.* **108**, 243601 (2012).
- [55] V. E. Lembessis, D. Ellinas, M. Babiker, and O. Al-Dossary, *Phys. Rev. A* **89**, 053616 (2014).
- [56] N. Radwell, T. W. Clark, B. Piccirillo, S. M. Barnett, and S. Franke-Arnold, *Phys. Rev. Lett.* **114**, 123603 (2015).
- [57] S. Sharma and T. N. Dey, *Phys. Rev. A* **96**, 033811 (2017).
- [58] H. R. Hamedī, V. Kudriašov, J. Ruseckas, and G. Juzeliūnas, *Opt. Express* **26**, 28249 (2018).
- [59] H. R. Hamedī, J. Ruseckas, and G. Juzeliūnas, *Phys. Rev. A* **98**, 013840 (2018).
- [60] H. R. Hamedī, J. Ruseckas, E. Paspalakis, and G. Juzeliūnas, *Phys. Rev. A* **99**, 033812 (2019).
- [61] D. Moretti, D. Felinto, and J. W. R. Tabosa, *Phys. Rev. A* **79**, 023825 (2009).
- [62] F. Cardano, F. Massa, H. Qassim, E. Karimi, S. Slussarenko, D. Paparo, C. de Lisio, F. Sciarrino, E. Santamato, R. W. Boyd *et al.*, *Sci. Adv.* **1**, e1500087 (2015).
- [63] H. R. Hamedī, E. Paspalakis, G. Žlabys, G. Juzeliūnas, and J. Ruseckas, *Phys. Rev. A* **100**, 023811 (2019).
- [64] Y. Hong, Z. Wang, D. Ding, and B. Yu, *Opt. Express* **27**, 29863 (2019).
- [65] J. Qiu, Z. Wang, D. Ding, W. Li, and B. Yu, *Opt. Express* **28**, 2975 (2020).
- [66] I. D. Maleev and G. A. Swartzlander, *J. Opt. Soc. Am. B* **20**, 1169 (2003).
- [67] E. J. Galvez, N. Smiley, and N. Fernandes, *Proc. SPIE* **6131**, 613105 (2006).
- [68] S. M. Baumann, D. M. Kalb, L. H. MacMillan, and E. J. Galvez, *Opt. Express* **17**, 9818 (2009).
- [69] A. Mair, A. Vaziri, G. Weihs, and A. Zeilinger, *Nature (London)* **412**, 313 (2001).
- [70] I. V. Basistiy, V. V. Slyusar, M. S. Soskin, M. V. Vasnetsov, and A. Y. Bekshaev, *Opt. Lett.* **28**, 1185 (2003).
- [71] W. M. Lee, B. P. S. Ahluwalia, X.-C. Yuan, W. C. Cheong, and K. Dholakia, *J. Opt. A: Pure Appl. Opt.* **7**, 1 (2005).
- [72] X. Z. H. Wang, *Opt. Commun.* **403**, 358 (2017).
- [73] M. G. Payne and L. Deng, *Phys. Rev. A* **64**, 031802(R) (2001).